1. RESIDUAL MONTE CARLO TREATMENT OF THE TIME VARIABLE

Another extension and improvement for the HOLO method described in Sec. **??** is the time discretization of the transport equation. We have incorporated the time variable into the ECMC method to improve efficiency over IMC, while still preserving the accuracy of MC integration. The main area of interest is in producing more accurate resolution of radiation wave-fronts in optically thin regions, where particles transport a long distance over a time step. In such regions, the MC integration of the time variable by IMC can produce greater accuracy than an implicit Euler discretization, which can produce artificially fast propagation of radiation in space. A potential application where this accuracy is important is stellar atmosphere calculations. It is noted that no adaptive refinement in time is performed, so maintaining exponential convergence may not be possible. However, we still expect the residual MC formulation of the ECMC method to show improvement in efficiency over standard MC.

In the remainder of this chapter, the inclusion of the time variable into the ECMC trial space is detailed, along with modifications to particle tracking and the ECMC algorithm. The process of sampling, tracking, and tallies particle histories in time is detailed in literature[**?**, 1, **?**, **?**], but sufficient details are provided in this chapter. Finally, a new temporal closure for the LO equations is given, and results are compared to IMC for accuracy and efficiency.

1.1 Modifications to the HO equations

Inclusion of the time variable t in the trial space used by ECMC allows for no discretization of the transport operator $\mathbf{L}$. The transport operator, applied to the

continuous intensity I, becomes

$$\mathbf{L}I(x,\mu,t) = \frac{1}{c}\frac{\partial I}{\partial t} + \mu\frac{\partial I}{\partial x} + \sigma_t I \tag{1.1}$$

The emission source is still treated with an implicit Euler discretization, which is similar to the approximation made in IMC. The ECMC algorithm specified in Sec. **??** does not need to be modified. However, the residual source and trial-space representation are modified to include t. Each batch is still estimating the error in the current projection estimate $\tilde{I}(x,\mu,t)$, but the time variable must be included in the inversion of the $\mathbf{L}$ operator.

1.1.1 The Doubly-Discontinuous Trial Space in Time

It is necessary to define a new trial space that includes the time variable so that we can explicitly evaluate the residual. The time variable has a similar representation to the LDD trial space used for the spatial variable in Sec. **??**, but the solution is a constant value over the interior of the time step. This step, doubly-discontinuous (SDD) trial space is defined as

$$\tilde{I}(x,\mu,t) = \begin{cases} \tilde{I}^n(x,\mu) & t = t^n \\ \overline{I}(x,\mu) & t \in (t^n, t^{n+1}) \\ \tilde{I}^{n+1}(x,\mu) & t = t^{n+1} \end{cases} \tag{1.2}$$

where we have used $\overline{I}$ to denote the time-averaged LDFE *projection* in x and μ of the intensity over the interior of the time step; the beginning and end of time step projections are denoted $\tilde{I}^n$ and $\tilde{I}^{n+1}$, respectively. An illustration of t for the SDD trial space, over the n-th time step, is depicted in Fig. 1.1. There is a projection error in using the LDFE projection to represent the intensity between time steps. However,

with sufficient noise reduction and mesh resolution, this should be an acceptable error compared to the large statistical noise of standard MC.

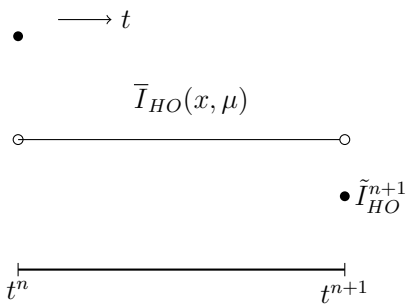

Figure 1.1: Step doubly-discontinuous representation of t for the HO solution.

The SDD trial space provides a projection for all the desired unknowns to exactly produce the moment equations, i.e., the time-averaged, end of time step, and previous time step intensities; temporally, these are the only unknowns that appear in equations that have been integrated over a time step to produce a balance statement. Another benefit of this trial space is it allows for infrastructure for computing the residual from the time-discrete case to be used directly. This trial space has one major drawback: only particle histories that reach t^{n+1} contribute to the estimation of $\tilde{\epsilon}^{n+1}$, and thus I^{n+1}. This is undesirable in optically thick problems.

REWRITE: Possibly move this to the future work section Alternatively, an LDFE representation could be used in the time variable. The linear representation would produce less noise because all particle tracks contribute to the slope, rather than just those that reach the end of the time step, although it would produce an approximate projection error for the end of time step intensity that is not produced with a discontinuity at the end of the time step. The linear representation in time would also

produce a more accurate reconstruction of the scattering source in time. However, a linear representation requires the sampling algorithm to be significantly modified because the L_1 integral for computing the residual magnitude is now significantly complicated by the tri-linear function. A possible way to sample this source is discussed in Appendix??? for completeness, but it has not been rigorously investigated.

1.1.2 Residual Source Definition and Sampling

The residual is defined as $r = q - \mathbf{L}\tilde{I}(x, \mu, t)$, where

$$q = \left(\sigma_a ac(T_{LO}^{n+1})^4(x) + \sigma_s \overline{\phi}_{LO}\right) \tag{1.3}$$

is a constant in time and provided by the LO solver. We have assumed a constant reconstruction for the scattering source in time. Evaluation of the residual with Eq. (1.2) for I produces a uniform source in time, as well as a δ-function source at the beginning and end of the time step. We write the residual source in terms of three components:

$$r(x, \mu, t) = \overline{r}(x, \mu) + r^n(x, \mu)\delta^+(t - t^n) + r^{n+1}(x, \mu)\delta^-(t - t^{n+1}), \quad t \in [t^n, t^{n+1}] \tag{1.4}$$

We will look at each component individually. The first residual term is a constant in time with representation

$$\overline{r}(x, \mu) = q - \mu \frac{\partial \overline{I}(x, \mu)}{\partial x} - \sigma_t \overline{I}(x, \mu) \tag{1.5}$$

Evaluation of the above function produces both face and volumetric sources, similar to in the discrete case. To sample x and μ from the face and volume distributions, the same rejection procedure can be used as for Eq. (**??**) and detailed in [3]. The

time variable can then be sampled uniformly over the time step, i.e., $t = t^n + \eta\Delta t$, where η is a uniform random variable with support $(0, 1)$.

The second source has definition

$$r^n(x,\mu) = -\frac{1}{c}\frac{\partial \overline{I}(x,\mu)}{\partial t}\bigg|_{t=t^n} = -\frac{1}{c}\left(\overline{I}(x,\mu) - \tilde{I}^n(x,\mu)\right) \tag{1.6}$$

This source is a LDFE space and angle volumetric source. The rejection sampling procedure is used to sample x and μ. All particles sampled from this source begin tracking with $t = t^n$.

The final source term is

$$r^{n+1}(x,\mu) = -\frac{1}{c}\frac{\partial \overline{I}(x,\mu)}{\partial t}\bigg|_{t=t^{n+1}} = -\frac{1}{c}\left(\tilde{I}^{n+1}(x,\mu) - \overline{I}(x,\mu)\right). \tag{1.7}$$

The source r^{n+1} can be treated using the same analytic treatment as the outflow face source in the LDD trial space, detailed in Sec. **??**; the source at the end of the time step is never sampled because its contribution to I^{n+1} can be analytically computed. To treat the sources this way, the solution for $\tilde{I}^{n+1}(x,\mu)$ is initialized to the value of $\overline{I}(x,\mu)$ before a batch of particles begins. Then, error particles that reach the end of the time step, referred to as "census" particles, contribute a standard score to the projection $\tilde{I}^{n+1}(x,\mu)$.

With these definitions, it is thus only necessary to sample from two sources. Using composite-rejection sampling [4], a discrete probability distribution is sampled to determine which source component to sample, followed by sampling of that component. The algorithm is

1. Sample uniform random number η
2. If $\eta < \|r^n\|_1/(\|r^n\|_1 + \|r^{n+1}\|_1)$:

- Sample from r^n source using rejection sampling
- Sample t uniformly over (t^n, t^{n+1}).

3. Else:
   - Sample from $\overline{r}$ source

All L_1 integrals can be analytically integrated using the same numerics as in the time-discrete case. The systematic sampling algorithm, as described in Sec. **??**, can be applied similarly. However, the choice of source is only make locally over that space-angle element. In that case, the element is chosen systematically, then the choice of r^n or $\overline{r}$ is sampled. REWRITE: Only discuss sampling of systematic case.

1.1.3 Importance Sampling on Interior of Time Step

As an attempt to reduce variance in the estimate of $\tilde{\epsilon}^{n+1}(x, \mu)$, we use important sampling in the time variable. Systematic sampling is still used for determining the cell of interest, and sampling as described above is used to determine which source is sampled, based on the appropriate probabilities described in the previous section. However, when the interior source $\overline{r}(x, \mu)$ is sampled, we use importance sampling for the conditional sampling of the uniform time step. The goal is to ensure that some histories reach the end of the time step. In order to do this, we sample from a modified PDF such that a fraction p_{end} of particles sampled from $\overline{r}(x, \mu)$ are born with $t \in (t^{end}, t^{n+1})$. We define $t^{end} = t^{n+1} - M/(c\sigma_t)$, where M is the desired number of MFP of travel the particle will undergo from the end of the time step (e.g., 2 or 3). The weights of particles sampled from this distribution must be modified to prevent source biasing.

The new PDF to be sampled from is

$$f^*(t) = \begin{cases} \frac{1-p_{end}}{t^{end}-t^n} & 0 < t < t^{end} \\ \frac{p_{end}}{t^{n+1}-t^{end}} & t^{end} \leq t < t^{n+1} \\ 0 & \text{elsewhere} \end{cases} \tag{1.8}$$

The original PDF is $f(t) = 1/\Delta t$, for $t \in (t^n, t^{n+1})$. Thus, using the standard procedure for importance sampling[4], the starting time t_{start} is sampled from $f^*(t)$, and then weights are multiplied by the factor $f(t_{\text{start}})/f^*(t_{\text{start}})$. This procedure is not perfect in that if a particle is moving from an optically thin to an optically thick region, it is not guaranteed to reach census. However, this case does not introduce bias.

1.1.4 Tracking and Tallying in Time

Because our LO equations will be integrated over the time step, we only need to perform MC tracking for $t \in [t^n, t^{n+1}]$. The initial time for the particle is sampled as described in the previous section. In inverting the $\mathbf{L}$ operator, particles are tracked until they reach the end of the time step. Path lengths are sampled or the weight is exponentially attenuated as before (e.g., Sec. **??**). As a particle travels from position x_o to x_f, with direction μ, the time is updated as

$$t^f = t^0 + \frac{|x_f - x_o|}{c\mu} \tag{1.9}$$

where c is the speed of light. For analog path-length sampling, if $t^f > t^{n+1}$ then t^f is adjusted to t^{n+1} and the path length is adjusted accordingly. For continuous weight deposition, particles are only tracked until they reach t^{n+1}. A proof that this process of tracking particles is a MC solution to an integral equation that is exactly inverse

to the **L** operator is detailed in [**?**, **?**].

Tallies must be adjusted to account for the averaging over the time step, and to compute the intensity at the end of time step. To produced the time-averaged representation $\overline{I}(x,\mu)$, requires estimators for the average, x, and μ moments of the error, e.g.,

$$\overline{\epsilon}_{x,ij} = \frac{1}{\Delta t}\frac{6}{h_j}\int_{t^n}^{t^{n+1}}\mathrm{d}t\int_{x_{i-1/2}\,\mu_{j-1/2}}^{x_{i+1/2}\,\mu_{j+1/2}}\mathrm{d}x\int\mathrm{d}\mu\,\left(\frac{x-x_j}{h_i}\right)\epsilon(x,\mu,t) \tag{1.10}$$

with a similar definition for the average and μ moments. The estimators are defined as

$$\hat{\overline{\epsilon}}_{x,ij} = \frac{1}{N_{hist}}\frac{6}{\Delta t h_i}\sum_{n=1}^{N_{hist}}\frac{s_n}{h_i h_j}w_j\left(x_c - x_i\right), \tag{1.11}$$

where the magnitude of the weights produce the L_1 integral over all phase space, i.e.,

$$\sum_{n=1}^{N} w_n = \|r(x,\mu,t)\|_1 \equiv \int_{t^n}^{t^{n+1}}\mathrm{d}t\int_{x_{i-1/2}\,\mu_{j-1/2}}^{x_{i+1/2}\,\mu_{j+1/2}}\mathrm{d}x\int\mathrm{d}\mu\,|r(x,\mu,t)|. \tag{1.12}$$

Here, x_c is the center of the n-th path length, and s_n is the path length for the n-th path length in the $x-\mu$ cell.

Moments of $I^{n+1}(x,\mu)$ must be estimated to represent the end of time step intensity. For example, the x moment for the ij-th cell of the error at the end of time step is

$$\epsilon_{x,ij}^{n+1} = \frac{6}{h_i}\iint_{\mathcal{D}_{ij}}\left(\frac{x-x_i}{h_i}\right)\epsilon(x,\mu,t^{n+1})\mathrm{d}x\mathrm{d}\mu \tag{1.13}$$

The estimators for these moments are a generalization of the census tallies used in IMC [**?**, **?**]. The tallies are based on the definition of the intensity as $I(x,\mu,t) = ch\nu N(x,\mu,t)$ given in Eq. (**??**), similar to collision estimators [4, **?**]. The census

estimator for the x moment is

$$\hat{\epsilon}_{x,ij}^{n+1} = \frac{1}{N_{hist}} \frac{6}{h_j h_i} \sum_{n=1}^{N_{hist}} cw_j \left(x_c - x_i\right) \tag{1.14}$$

Similar tallies are defined for the other space-angle moments. These tallies can be exceptionally noisy because only particles that reach the end of the time step contribute.

1.2 Closing the LO Equations in Time

The LO equations must be closed in time consistently with the HO equations. Previous work has enforced consistency in time by adding a local artificial source to the time-discretized LO equations in each cell [7]. This source was approximated based on the difference between the exact HO integral of the time derivative and the approximate representation in the LO equations. The advantage of this form is that the LO solver exclusively deals in time-averaged unknowns for the radiation terms in the equations. However, if the problem is strongly non-linear or the time-averaged and time-edge values differ greatly, this may become unstable.

We will alternatively use a parametric closure in the time variable, similar to the spatial closures discussed in the Sec. **??**. The time-integrated LO equations can be written exclusively in terms of time-averaged unknowns. This closure produces LO equations that have the same numerical difficulty to solve as the BE, fully-discrete LO equations, but have the potential to preserve the accuracy of the MC integration in time, upon non-linear convergence of the system. A closure relation is used to eliminate the end of time step moments present from the time derivative term. We will investigate different parametric forms of the closure for robustness. Once the time-averaged unknowns have been calculated, the time closures can be used to convert the time-averaged unknowns to end-of-time-step values.

REWRITE THIS SENTENCE One potential benefit of the time closure parameters is that $\overline{I}^{HO}$ will be most different from $I^{HO,n+1}$ in problems that are optically thin. In such problems, σ_a is small, leading to an optically thin problem. However, there may be difficulties in the MPV problems where the problems are tightly coupled and nonlinear, but can lead to a large change over a time step.

REWRITE: I think most of these paragraphs can be moved to intro

1.2.1 Derivation of Time-Averaged Moment Equations

The time-continuous radiation equations are integrated in space and angle the same as before. For example, the L and $+$ moment equation is

$$\frac{1}{c}\frac{\partial}{\partial t}\langle\phi\rangle_L^+ - 2\left(\mu_{i-1/2}I_{i-1/2}\right)^+ + \langle\mu I\rangle_{L,i}^+ + \langle\mu I\rangle_{R,i}^+ + \sigma_{t,i}h_i\langle\phi\rangle_{L,i}^+ - \frac{\sigma_{s,i}h_i}{2}\left(\langle\phi\rangle_{L,i}^+ + \langle\phi\rangle_{L,i}^-\right) = \frac{h_i}{2}\langle\sigma_a acT^4\rangle_{L,i} \quad (1.15)$$

This equation is then integrated over the time step, and the emission source is assumed implicit. The same manipulations can be performed on the streaming term to form angular consistency terms, but the weighting fluxes are now time-averaged values. Thus, the angular consistency terms are computed with $\overline{I}(x,\mu)$. The equations with time-averaged consistency terms are

$$\frac{\langle\phi\rangle_{L,i}^{+,n+1} - \langle\phi\rangle_{L,i}^{+,n}}{c\Delta t} - 2\overline{\mu}_{i-1/2}^+\overline{\phi}_{i-1/2}^+ + \overline{\{\mu\}}_{L,i}^+\langle\overline{\phi}\rangle_{L,i}^+ + \overline{\{\mu\}}_{R,i}^+\langle\overline{\phi}\rangle_{R,i}^+ + \sigma_{t,i}^{n+1}h_i\langle\overline{\phi}\rangle_{L,i}^{n+1,+} - \frac{\sigma_{s,i}h_i}{2}\left(\langle\overline{\phi}\rangle_{L,i}^+ + \langle\overline{\phi}\rangle_{L,i}^-\right) = \frac{h_i}{2}\langle\sigma_a^{n+1}acT^{n+1,4}\rangle_{L,i}, \quad (1.16)$$

These equations are exact at this point. The BE approximation is used for the temperature terms in the material energy equations, but the radiation energy deposition is a time-averaged valued. REWRITE: Maybe add material energy equation

1.2.2 Parametric Time Closure

The closure relations in time are different than the closure relations for the spatial variable because we do not have a slope in time. The following closure is a modified diamond relation:

$$I^{n+1} = 2\gamma\overline{I} - I^n \tag{1.17}$$

where γ is the closure factor and $\overline{I}$ is the time-averaged intensity. A modified BE discretization can also be used:

$$I^{n+1} = \gamma\overline{I} \tag{1.18}$$

The chosen closure relation must be used to eliminate the unknowns at t^{n+1} from each of the LO moment equations, with the values from the previous time step taken as a known quantity. Thus, it is necessary to have a closure relation for each moment and half range, producing four closure parameters per spatial cell. The closure relations for the L moment and the modified diamond relation are

$$\langle\phi\rangle_{L,i}^{\pm,n+1} = 2\gamma_{L,i}^{\pm}\langle\overline{\phi}\rangle_{L,i}^{\pm} - \langle\phi\rangle_{L,i}^{\pm,n} \tag{1.19}$$

with equivalent definitions for the R moment. Substitution of the above equation into Eq. (1.16)

$$\frac{2}{c\Delta t}\left[\gamma_{L,i}^{+}\langle\phi\rangle_{L}^{+,n+1} - \langle\phi\rangle_{L}^{+,n}\right] - 2\overline{\mu}_{i-1/2}^{+}\overline{\phi}_{i-1/2}^{+} + \overline{\{\mu\}}_{L,i}^{+}\langle\overline{\phi}\rangle_{L,i}^{+} + \overline{\{\mu\}}_{R,i}^{+}\langle\overline{\phi}\rangle_{R,i}^{+} + \sigma_{t,i}^{n+1}h_i\langle\overline{\phi}\rangle_{L,i}^{n+1,+} - \frac{\sigma_{s,i}h_i}{2}\left(\langle\overline{\phi}\rangle_{L,i}^{+} + \langle\overline{\phi}\rangle_{L,i}^{-}\right) = \frac{h_i}{2}\langle\sigma_a^{n+1}acT^{n+1,4}\rangle_{L,i}, \tag{1.20}$$

The other moment equations are analogously defined.

The value of $\gamma_{L,i}^{+}$, $\gamma_{R,i}^{+}$, $\gamma_{L,i}^{-}$, and $\gamma_{R,i}^{-}$ can be computed by substituting the trial-space representation of $I^{HO}(x,\mu,t)$ into Eq. (1.19) and its analogs.

1.3 Computational Results

We will test the time-closure in several characteristic cases. The first case is a near-void where the time-closure parameters will provide the most correction compared to a Backward Euler discretization. The second problem is the Marshak wave problem from Sec. **??**. This problem is optically thick, so minimal time-correction is needed, but there will likely be higher variance in the tallies. We will compare to IMC visually for accuracy to determine that we are converging towards the correct solution. For the near void case the IMC solution is accurate because the material energy equation is uncoupled.

When negative averages occur, they are set to the floor value. Causality is not strictly preserved because you are sampling the error, so it is possible to have particles out front of the wave front.

1.3.1 Near-Void Problem

The problem specifics for this problem are a constant. We use the systematic sampling algorithm and no biasing in time as the problem is optically thin. The material properties are uniform throughout the 2.0 cm domain with $\rho c_v = 0.01374$ Jks cm^{-3} keV^{-1}, $\sigma_a = 10^{-6}$ cm^{-1}, and $\sigma_s = 0$ cm^{-1}. The material and radiation are initially in equilibrium at a temperature of 0.01 keV. An isotropic incident intensity of 0.150 keV is applied at $x = 0$; the incident intensity on the right boundary is 0.01 keV. The simulation end time is 0.003 sh.

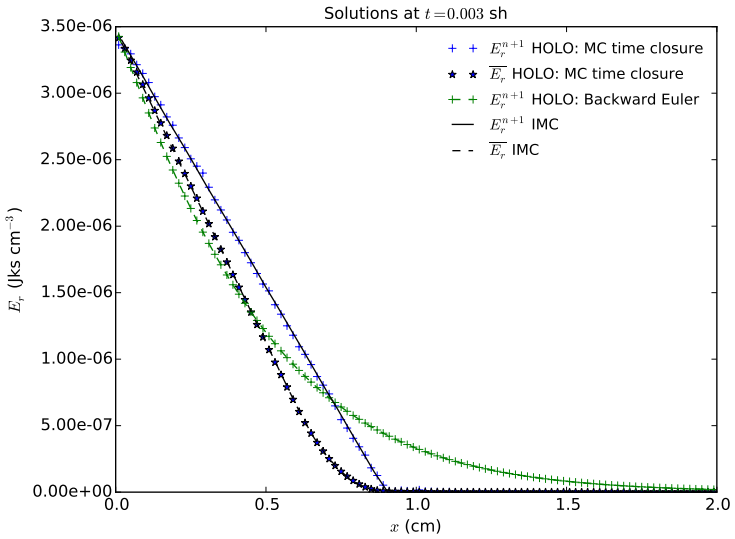

Figure 1.2: Comparison of radiation energy densities of IMC and HOLO method for the MC time closure and a BE discretization.

A comparison of the cell-averaged radiation energy densities E_r for IMC, the HOLO method with HO time closure, and the HOLO method with time-discrete equations are shown in Fig **??**. For the HOLO results, three ECMC batches were performed with a total of 3×10^6 histories per time step and the IMC results performed 12×10^6 histories per time step.

A comparsion for radiation temperatures with 1 and 3 batches is given in Fig. **??**, which reveals that there is substantial noise past the wave front for the 3 batches case. This noise is small relative to the scale of the solution in the wave-front, which is why it is not visible in the mean intensity plots. This demonstrates one deficiency in this methdo that particles sampled near the wave-front can potentially ahve a time near the beginning of the time step and travel into the equilibrium region. The solution is not biased however, if sufficient samplign was performed there woudl be negative particles that canceled out this error. The residual MC case does not display

this error as drastically because the guessed solution takes on the form of the old solution, particles can not transport past what physics allows, with the exception of some smearing due to the projection error incurred between time steps.

We have computed FOM statistics using Eq. (**??**) with 20 independent runs for each configuration. In general more particle histories are needed to produce an accurate result.

Table 1.1: **Comparison of sample statistics for the Near-Void problem. Simulation end time is t = 0.003 sh.**

	ß		FOM	
hists./step	IMC	HOLO-ECMC	IMC	HOLO-ECMC
300,000 1,000,000	3.40%	0.28%	1	145
2,000,000	1.22%	0.057%	0.93	422

REFERENCES

[1] J. A. Fleck, Jr. and J. D. Cummings, Jr. An implicit monte carlo scheme for calculating time and frequency dependent nonlinear radiation transport. *J. Comput. Phys.*, 8(3):313–342, December 1971.

[2] Elmer Eugene Lewis and Warren F Miller. *Computational methods of neutron transport*. John Wiley and Sons, Inc., New York, NY, 1984.

[3] J.R. Peterson. Exponentially Convergent Monte Carlo for the 1-d Transport Equation. Master's thesis, Texas A&M, 2014.

[4] J.K. Shultis and W.L. Dunn. *Exploring Monte Carlo Methods*. Academic Press, Burlington, MA 01803, 2012.

[5] "Weston M. Stacey". *"Nuclear Reactor Physics"*. Wiley, 2007.

[6] T.A. Wareing. *Asymptotic diffusion accelerated discontinuous finite element methods for transport problems*. PhD thesis, Michigan, 1991.

[7] Allan B. Wollaber, H. Park, R.B. Lowrie, R.M. Rauenzahn, and M.E. Cleveland. Radiation hydrodynamics with a high-order, low-order method. In *ANS Topical Meeting, International Topical Meeting on Mathematics and Computation*, Nashville Tennessee, 2015.

APPENDIX A

DERIVATIONS AND EQUATIONS FOR THE LO SYSTEM

A.1 Useful Moment Relations for LO Equations

There are several relations between various moment definitions that are useful in derivation and manipulation of the LO equations. The following are derived for $\phi(x)$, but can be applied to general moments of functions. The volumetric average terms can be eliminated in terms of the L and R moments from the relation $b_{L,i}(x) + b_{R,i}(x) = 1$.

$$\phi_i = \frac{1}{h_i} \int_{x_{i-1/2}}^{x_{i+1/2}} 1 \, \phi(x) \mathrm{d}x \tag{A.1}$$

$$= \frac{1}{h_i} \left(\int_{x_{i-1/2}}^{x_{i+1/2}} b_{L,i}(x)\phi(x)\mathrm{d}x + \int_{x_{i-1/2}}^{x_{i+1/2}} b_{R,i}(x)\phi(x)\mathrm{d}x \right) \tag{A.2}$$

$$= \frac{1}{2} \left(\langle \phi \rangle_{L,i} + \langle \phi \rangle_{R,i} \right) \tag{A.3}$$

A similar relation can be derived for the first moment in space as

$$\phi_{x,i} = \frac{3}{2} \left(\langle \phi \rangle_{R,i} - \langle \phi \rangle_{L,i} \right) \tag{A.4}$$

The above relations can be inverted to derived a relation for the L and R moments in terms of the slope and average moments. These moment expressions are defined purely in terms of integrals, and are independent of the chosen spatial representation

Once a linear relation on the interior has been assumed, there are other useful closures that can be derived. The standard linear interpolatory expansion, for the

positive half-range, is restated here:

$$\phi^+(x) = \phi^+_{L,i} b_{L,i}(x) + \phi^+_{R,i} b_{R,i}(x) \tag{A.5}$$

Using this expansion, one can derive a relation between the outflow from a cell and the hat function moments that is equivalent to the standard LDFE Galerkin method:

$$\phi^+_{i,R} = 2\langle\phi\rangle^+_{R,i} - \langle\phi\rangle^+_{L,i} \tag{A.6}$$

this linear relation also defines the value for $\phi^+_{i,L}$.

To eliminate the LO unknowns in a manner that is equivalent to lumping the discrete system, the following expression can be used for the outflow from a cell

$$\phi^+_{i+1/2} = \phi^+_i + \frac{\phi^+_x}{3}, \tag{A.7}$$

which in terms of the hat function moments is equivalent to $\phi^+_{i+1/2} = \langle\phi\rangle^+_{R,i}$. Inserting this expression into Eq. (**??**), and using the same definition for the linear representation over the interior of $\phi^+_{i+1/2}(x) = \phi_{L,i} b_{L,i}(x) + \phi_{R,i} b_{R,i}(x)$, will produce an equivalent set of unknowns as a linear discontinuous method with a lumped representation for the radiation. The temperature equation must be independently lumped. This relation preserves the average within a cell but modifies the first moment.

A similar expression produces a lumped-equivalent representation on the interior of the cell:

$$\phi^+_{i,R} = \phi^+_i + \frac{\phi^+_x}{3}, \tag{A.8}$$

The moment equations are not modified by using this expression, however the interpretation of the moments as a linear representation over the cell has been altered.

This allows for us to ensure a lumped representation on the interior while still using the HO solution to eliminate the outflow from the equations.

A.2 Newtons Method for the LO Equations

Because we have only considered problems with constant densities and heat capacities, the linearization described below is in terms of temperature T rather than material internal energy, for simplicity. However, the linearization can be formed in terms of internal energy to apply this method to a general equation of state.

To formulate the Newton iterations, the Planckian source is linearized in the material and radiation equations (Eq. (**??**) & Eq. (**??**)). Application of the first order Taylor expansion in time to the implicit emission source $B(T^{n+1})$, about some temperature T^* at some time $t^* \in [t^n, t^{n+1}]$, yields

$$\sigma_a^{n+1} acT^{4,n+1} \simeq \sigma_a^* ac \left[T^{*4} + (T^{n+1} - T^*)4T^{*3}\right] \tag{A.9}$$

where $\sigma_a^* \equiv \sigma_a(T^*)$. Substitution of this expression into Eq. (**??**) yields

$$\rho c_v \left(\frac{T^{n+1} - T^n}{\Delta t}\right) = \sigma_a^* \phi^{n+1} - \sigma_a^* ac \left[T^{*4} + (T^{n+1} - T^*)4T^{*3}\right]. \tag{A.10}$$

Algebraic manipulation of this equation yields an expression for $T^{n+1} - T^*$:

$$\left(T^{n+1} - T^*\right) = \frac{\frac{\sigma_a^* \Delta t}{\rho c_v}\left[\phi^{n+1} - acT^{*4}\right] + (T^n - T^*)}{1 + \sigma_a^* ac\Delta t \frac{4T^{*3}}{\rho c_v}}.$$

This expression is substituted back into Eq. (A.9) to form an explicit approximation for the emission source at t^{n+1} as

$$\sigma_a acT^{4,n+1} \simeq \sigma_a^*(1 - f^*)\phi^{n+1} + f^* \sigma_a^* acT^{4,n} + \rho c_v \frac{1 - f^*}{\Delta t}(T^n - T^*) \tag{A.11}$$

where $f^* = [1 + \sigma_a^* c\Delta t 4aT^{*3}/(\rho c_v)]^{-1}$ is often referred to as the Fleck factor [1].

Next, the above equation must be spatially discretized. Application of the L spatial moment yields

$$\langle \sigma_a^* acT^{4,n+1} \rangle_{L,i} = \sigma_{ai}^*(1 - f_i^*)\langle \phi^{n+1} \rangle_{L,i} + f_i^* \sigma_{ai}^* ac \left(\frac{2}{3} T_{L,i}^{4,n} + \frac{1}{3} T_{R,i}^{4,n} \right) \\ \rho_i c_{vi} \frac{1 - f_i^*}{\Delta t} \left[\frac{2}{3} \left(T_{L,i}^n - T_{L,i}^* \right) + \frac{1}{3} \left(T_{R,i}^n - T_{R,i}^* \right) \right], \quad \text{(A.12)}$$

where $T^{4,n}$ and T^n have been assumed LD and f^* is assumed constant over a cell, i.e., $f_i^* \equiv \sigma_a(T_i^*)$. The error introduced by a constant f^* approaches zero as the non-linearity is converged because T^* approaches T^{n+1}. Based on an estimate for T^*, Eq. (A.12) is an expression for the Planckian emission source in the radiation moment equations with an additional effective scattering source. A similar expression can be derived for $\langle \sigma_{a,i} acT^4 \rangle_R$ and the right moment equations. The expressions for the emissions source is substituted into the radiation moment equations (Eq. (**??**)–(**??**)) to produce a linear system of equations for the new radiation intensity moments.

Once the linear equations have been solved for new radiation moments, new temperature unknowns can be estimated. To conserve energy, the same linearization and discretizations used to solve the radiation equation must be used in the material energy equation. Substitution of Eq. (A.12) into the material energy L moment equation ultimately yields

$$\frac{2}{3} T_{L,i}^{n+1} + \frac{1}{3} T_{R,i}^{n+1} = \frac{f_i^* \sigma_{ai}^* \Delta t}{\rho c_v} \left[\langle \phi^{n+1} \rangle_{L,i} - ac \left(\frac{2}{3} T_{L,i}^{4,n} + \frac{1}{3} T_{R,i}^{4,n} \right) \right] + \\ (1 - f_i^*) \left(\frac{2}{3} T_{L,i}^* + \frac{1}{3} T_{R,i}^* \right) + f \left(\frac{2}{3} T_{L,i}^n + \frac{1}{3} T_{R,i}^n \right) \quad \text{(A.13)}$$

A similar expression is produced for the R moment equation. This produces a local

matrix equation to solve for new T unknowns. If both the radiation and temperature unknowns are lumped, this matrix becomes diagonalized.

Based on these equations, the algorithm for solving the LO equations, with iteration index l, is defined as

1. Initialize T unknowns using T^n or the last estimate of T^{n+1} from previous LO solve

2. Build the LO system based on the effective scattering $(1 - f^l)$ and emission terms evaluated using T^l.

3. Solve the linearized LO system to produce an estimate for $\phi^{n+1,l}$.

4. Evaluate a new estimate of T^{n+1} unknowns using Eq. (A.13).

5. $T^* \leftarrow \tilde{T}^{n+1}$.

6. Repeat 2-5 until $(T^{n+1,k})^4$ and $\phi^{n+1,k}$ are converged.

Figure A.1: TAMU figure

A.3 Derivation of the WLA-DSA Equations

In this section, we derive the discretized diffusion equation and LD mapping equations that are used in the WLA-DSA equations. To simplify notation, we derive the equations from a generic transport equation (rather than the error equations) with isotropic scattering and source q_0, i.e.,

$$\mu \frac{\partial I}{\partial x} + \sigma_t I = \frac{\sigma_s}{2} \left(\phi(x) + q_0 \right). \tag{A.14}$$

A.3.1 Forming a Continuous Diffusion Equation

First, a continuous spatial discretization of a diffusion equation is derived. The mean intensity ϕ will ultimately be assumed continuous at faces to produce a standard three-point finite-difference diffusion discretization. The zeroth and first μ moment of Eq. (A.14) produce the P_1 equations [2, 6], i.e.,

$$\frac{\partial J}{\partial x} + \sigma_a \phi = q_0 \tag{A.15}$$

$$\sigma_t J + \frac{1}{3}\frac{\partial \phi}{\partial x} = 0. \tag{A.16}$$

The spatial finite element moments (defined by Eq. (**??**) and (**??**)) are taken of the above equations. The mean intensity is assumed linear on the interior of the cell, i.e., $\phi(x) = \phi_L b_L(x) + \phi_R b_R(x)$, for $x \in (x_{i-1/2}, x_{i+1/2})$. Taking the left moment, evaluating integrals, and rearranging yields

$$J_i - J_{i-1/2} + \frac{\sigma_{a,i} h_i}{2}\left(\frac{2}{3}\phi_{L,i} + \frac{1}{3}\phi_{R,i}\right) = \frac{h_i}{2}\langle q \rangle_{L,i} \ , \tag{A.17}$$

where J_i is the average of the flux J over the cell. The moments of q are not simplified to be compatible with the error equations which are in terms of moments. For the R moment

$$J_{i+1/2} - J_i + \frac{\sigma_{a,i} h_i}{2}\left(\frac{2}{3}\phi_{L,i} + \frac{1}{3}\phi_{R,i}\right) = \frac{h_i}{2}\langle q \rangle_{R,i} \ . \tag{A.18}$$

The equation for the L moment is evaluated for cell $i+1$ and added to the R moment equation evaluated at i. The flux J is assumed continuous at $i + 1/2$ to eliminate the face fluxes from the equations. The sum of the two equations becomes

$$J_{i+1} - J_i + \frac{\sigma_{a,i+1} h_{i+1}}{2}\left(\frac{2}{3}\phi_{L,i+1} + \frac{1}{3}\phi_{R,i+1}\right) + \frac{\sigma_{a,i} h_i}{2}\left(\frac{1}{3}\phi_{L,i} + \frac{2}{3}\phi_{R,i}\right) =$$

$$\frac{h}{2}\left(\langle q\rangle_{L,i+1}+\langle q\rangle_{R,i}\right). \quad \text{(A.19)}$$

The mean intensity is approximated as continuous at each face, i.e., $\phi_{L,i+1}=\phi_{R,i}\equiv\phi_{i+1/2}$. Adding the L and R moments of Eq. (A.16) together, with the continuous approximation for $\phi_{i+1/2}$, produces a discrete Fick's law equation [5]

$$J_i=-D_i\frac{\phi_{i+1/2}-\phi_{i-1/2}}{h_i}, \quad \text{(A.20)}$$

where $D_i=1/(3\sigma_{t,i})$. Substitution of Eq. (A.20) into Eq. (A.19) and rearranging yields the following discrete diffusion equation:

$$\left(\frac{\sigma_{a,i+1}h_{i+1}}{6}-\frac{D_{i+1}}{h_{i+1}}\right)\phi_{i+3/2}+\left(\frac{D_{i+1}}{h_{i+1}}+\frac{D_i}{h_i}+\frac{\sigma_{a,i+1}h_{i+1}}{3}+\frac{\sigma_{a,i}h_i}{3}\right)\phi_{i+1/2}$$
$$+\left(\frac{\sigma_{a,i}h_i}{6}-\frac{D_i}{h_i}\right)\phi_{i-1/2}=\frac{h_{i+1}}{2}\langle q\rangle_{L,i+1}+\frac{h_i}{2}\langle q\rangle_{R,i}\ . \quad \text{(A.21)}$$

To allow for the use of lumped or standard LD in these equations, we introduce the factor θ, with $\theta=1/3$ for standard LD, and $\theta=1$ for lumped LD. The diffusion equation becomes

$$\left(\frac{\sigma_{a,i+1}h_{i+1}}{4}(1-\theta)-\frac{D_{i+1}}{h_{i+1}}\right)\phi_{i+3/2}+\left(\frac{D_{i+1}}{h_{i+1}}+\frac{D_i}{h_i}+\left(\frac{1+\theta}{2}\right)\left[\frac{\sigma_{a,i+1}h_{i+1}}{2}+\frac{\sigma_{a,i}h_i}{2}\right]\right)\phi_{i+1/2}$$
$$+\left(\frac{\sigma_{a,i}h_i}{4}(1-\theta)-\frac{D_i}{h_i}\right)\phi_{i-1/2}=\frac{h_{i+1}}{2}\langle q\rangle_{L,i+1}+\frac{h_i}{2}\langle q\rangle_{R,i}\ . \quad \text{(A.22)}$$

Summation over all cells forms a system of equations for ϕ at each face.

A.3.1.1 Diffusion Boundary Conditions

The upwinding in the LO system exactly satisfies the inflow boundary conditions, therefore a vacuum boundary condition is applied to the diffusion error equations.

The equation for the left moment at the first cell is given by

$$J_1 - J_{1/2} + \frac{\sigma_{a,i} h_i}{2} \left(\frac{1+\theta}{2} \phi_{L,i} + \frac{1-\theta}{2} \phi_{R,i} \right) = \frac{h_i}{2} \langle q \rangle_{L,i} \ , \tag{A.23}$$

The Marshak boundary condition for the vacuum inflow at face $x_{1/2}$ is given as

$$J^+_{1/2} = 0 = \frac{\phi_{1/2}}{4} + \frac{J_{1/2}}{2}, \tag{A.24}$$

which can be solved for $J_{1/2}$. Substitution of the above equation and Eq. (A.20) into Eq. (A.23) gives

$$\left(\frac{1}{2} + \sigma_{a,1} h_1 \frac{1+\theta}{4} - \frac{D_1}{h_1} \right) \phi_{1/2} + \left(\sigma_{a,1} h_1 \frac{1-\theta}{4} - \frac{D_1}{h_1} \right) \phi_{3/2} = \frac{h_i}{2} \langle q \rangle_{L,1} \tag{A.25}$$

A similar expression can be derived for the right-most cell.

A.3.2 Mapping Solution onto LD Unknowns

Solution of the continuous diffusion equation will provide an approximation to ϕ on faces, denoted as $\phi^C_{i+1/2}$. We now need to map the face solution onto the LD representation of ϕ. To do this, first we take the L and R finite element moments of the P_1 equations. A LDFE dependence is assumed on the interior of the cell for J and ϕ. Taking moments of Eq. (A.15) and simplifying yields

$$J_{i+1/2} - \frac{J_{L,i} + J_{R,i}}{2} + \frac{\sigma_{a,i} h_i}{2} \left(\frac{1}{3} \phi_{L,i} + \frac{2}{3} \phi_{R,i} \right) = \frac{h_i}{2} \langle q \rangle_{R,i} \tag{A.26}$$

$$\frac{J_{L,i} + J_{R,i}}{2} - J_{i-1/2} + \frac{\sigma_{a,i} h_i}{2} \left(\frac{2}{3} \phi_{L,i} + \frac{1}{3} \phi_{R,i} \right) = \frac{h_i}{2} \langle q \rangle_{L,i} \tag{A.27}$$

The moment equations for Eq. (A.16) are

$$\frac{1}{3}\left(\phi_{i+1/2} - \frac{\phi_{i,L}+\phi_{i,R}}{2}\right) + \frac{\sigma_{t,i}h_i}{2}\left(\frac{1}{3}J_{L,i} + \frac{2}{3}J_{R,i}\right) = 0 \tag{A.28}$$

$$\frac{1}{3}\left(\frac{\phi_{i,L}+\phi_{i,R}}{2} - \phi_{i-1/2}\right) + \frac{\sigma_{t,i}h_i}{2}\left(\frac{2}{3}J_{L,i} + \frac{1}{3}J_{R,i}\right) = 0 \tag{A.29}$$

The face terms $J_{i\pm1/2}$ and $\phi_{i\pm1/2}$ need to be eliminated from the system. First, the scalar intensity is assumed to be the value provided by the continuous diffusion solution at each face, i.e., $\phi_{i\pm1/2} = \phi^C_{i\pm1/2}$. Then, the fluxes are decomposed into half-range values to decouple the equations between cells. At $x_{i+1/2}$, the flux is composed as $J_{i+1/2} = J^+_{i+1/2} + J^-_{i+1/2}$, noting that in this notation the half-range fluxes are $J^\pm_{i+1/2} = \pm\int_0^\pm \mu I(x_{i+1/2},\mu)\mathrm{d}\mu$[1]. We approximate the incoming fluxes, e.g., $J^-_{i+1/2}$, based on $\phi^C_{i+1/2}$ and a P_1 approximation. The P_1 approximation provides the following relation [6]

$$\phi = 2(J^+ - J^-). \tag{A.30}$$

At $x_{i+1/2}$, the above expression is solved for the incoming current $J^-_{i+1/2}$. The total current becomes

$$J_{i+1/2} = J^+_{i+1/2} - J^-_{i+1/2} = 2J^+_{i+1/2} - \frac{\phi^C_{i+1/2}}{2}, \tag{A.31}$$

In the positive direction, at the right face, the values of ϕ and J are based on the LD representation within the cell at that face, i.e., $\phi_{R,i}$ and $J_{R,i}$. The standard P_1 approximation for the half-range fluxes is used[5], i.e.,

$$J^\pm = \frac{\gamma\phi}{2} \pm \frac{J}{2}, \tag{A.32}$$

[1]Typically, the half-range fluxes are defined with integrals weighted with $|\mu|$, but this notation would not be consistent with our definition of the half-range consistency terms

where γ accounts for the difference between the LO parameters and the true P_1 approximation. Thus, for the right face and positive half-range,

$$J^+_{i+1/2} = \frac{\gamma}{2}\phi_{i,R} + \frac{J_{i,R}}{2} \tag{A.33}$$

A similar expression can be derived for $x_{i-1/2}$. The total fluxes at each face are thus

$$J_{i+1/2} = \gamma\phi_{i,R} + J_{i,R} - \frac{\phi^C_{i+1/2}}{2} \tag{A.34}$$

$$J_{i-1/2} = \frac{\phi^C_{i-1/2}}{2} - \gamma\phi_{i,L} + J_{i,L} \tag{A.35}$$

Substitution of these results back into the LD balance equations and introduction of the lumping notation yields the final equations

$$\left(\gamma\phi_{i,R} + J_{i,R} - \frac{\phi^C_{i+1/2}}{2}\right) - \frac{J_{L,i} + J_{R,i}}{2} + \frac{\sigma_{a,i}h_i}{2}\left(\frac{(1-\theta)}{2}\phi_{L,i} + \frac{(1+\theta)}{2}\phi_{R,i}\right) = \frac{h_i}{2}\langle q\rangle_{R,i} \tag{A.36}$$

$$\frac{J_{L,i} + J_{R,i}}{2} - \left(\frac{\phi^C_{i-1/2}}{2} - \gamma\phi_{i,L} + J_{i,L}\right) + \frac{\sigma_{a,i}h_i}{2}\left(\frac{(1+\theta)}{2}\phi_{L,i} + \frac{(1-\theta)}{2}\phi_{R,i}\right) = \frac{h_i}{2}\langle q\rangle_{L,i} \tag{A.37}$$

$$\frac{1}{3}\left(\phi^C_{i+1/2} - \frac{\phi_{i,L} + \phi_{i,R}}{2}\right) + \frac{\sigma_{t,i}h_i}{2}\left(\frac{(1-\theta)}{2}J_{L,i} + \frac{(1+\theta)}{2}J_{R,i}\right) = 0 \tag{A.38}$$

$$\frac{1}{3}\left(\frac{\phi_{i,L} + \phi_{i,R}}{2} - \phi^C_{i-1/2}\right) + \frac{\sigma_{t,i}h_i}{2}\left(\frac{(1+\theta)}{2}J_{L,i} + \frac{(1-\theta)}{2}J_{R,i}\right) = 0. \tag{A.39}$$

The above equations are completely local to each cell and fully defined, including for boundary cells. For simplicity, we just take $\gamma = 1/2$. The system can be solved for the desired unknowns $\phi_{i,L}$, $\phi_{i,R}$, $J_{i,L}$, and $J_{i,R}$, which represent the mapping of $\phi^C_{i+1/2}$

onto the LD representation for $\phi^{\pm}(x)$.

APPENDIX B

SECOND APPENDIX WITH A LONGER TITLE - MUCH LONGER IN FACT

Text for the Appendix follows.

Figure B.1: TAMU figure

B.1 Appendix Section